Elsevier Editorial System(tm) for Renewable Energy

Manuscript Draft

Manuscript Number: RENE-D-19-00704

Title: Turbulence-parameter Estimation for Current-energy Converters Using Surrogate Model Optimization

Article Type: Research Paper

Keywords: Actuator disc; OpenFOAM; Gaussian-process regression; Surrogate; Turbulence

Corresponding Author: Mr. Sterling Olson, MS

Corresponding Author's Institution:

First Author: Sterling Olson, MS

Order of Authors: Sterling Olson, MS; Jack C. P. Su; Humberto III Silva; Chris Chartrand; Jesse Roberts

Abstract: Surrogate models maximize information utility by building predictive models in place of computational or experimentally expensive model runs. Marine hydrokinetic current energy converters require large-domain simulations to estimate array efficiencies and environmental impacts. Meso-scale models typically represent turbines as actuator discs that act as momentum sinks and sources of turbulence and its dissipation. An OpenFOAM model was developed where actuator-disc k-ϵ turbulence was characterized using an approach developed for flows through vegetative canopies. Turbine-wake data from laboratory flume experiments collected at two influent turbulence intensities were used to calibrate parameters in the turbulence-source terms in the k-ϵ equations. Parameter influences on longitudinal wake profiles were estimated using Gaussian-process regression with subsequent optimization minimizing the objective function within 3.1\% of those those obtained using the full model representation, but for 74\% of the computational cost (far fewer model runs). This framework facilitates more efficient parameterization of the turbulence-source equations using turbine-wake data.

Suggested Reviewers: Craig Jones Ph.D
Principal, Integral Consulting
cjones@integral-corp.com
Craig is highly familiar with actuator disc environmental models. The application of this research would be to a group such as that run by Craig.

Daniel Appelö Ph.D
Associate Professor, Applied Mathematics, University of Colorado Boulder
Daniel.Appelo@Colorado.edu
Dr. Apello is familiar with CFD, and the math relevant to the surrogate model as well as the optimization process.

Carlos M Ströfer MS

Ph.D. Candidate, Aerospace and Ocean Engineering, Virginia Polytechnic Institute and State Univer
cmich@vt.edu
Carlos is familiar with CFD, Marine energy, and machine learning.

*Title Page

Turbulence-parameter Estimation for Current-energy Converters Using Surrogate Model Optimization

Sterling S. Olson[a,b,c], MS
Jack C. P. Su[b], Ph.D.
H. Silva III[c,d], Ph.D.
Chris C. Chartrand[a], MS
Jesse D. Roberts[a], MS
[a] *Sandia National Laboratories, Water Power Technologies Department, Albuquerque, NM, USA*
[b] *The University of New Mexico, Anderson School of Management, Albuquerque, NM, USA*
[c] *The University of New Mexico, Department of Mechanical Engineering, Albuquerque, NM, USA*
[d] *Sandia National Laboratories, Thermal Sciences & Engineering, Albuquerque, NM, USA*

Abstract

Surrogate models maximize information utility by building predictive models in place of computational or experimentally expensive model runs. Marine hydrokinetic current energy converters require large-domain simulations to estimate array efficiencies and environmental impacts. Meso-scale models typically represent turbines as actuator discs that act as momentum sinks and sources of turbulence and its dissipation. An OpenFOAM model was developed where actuator-disc k-ϵ turbulence was characterized using an approach developed for flows through vegetative canopies. Turbine-wake data from laboratory flume experiments collected at two influent turbulence intensities were used to calibrate parameters in the turbulence-source terms in the k-ϵ equations. Parameter influences on longitudinal wake profiles were estimated using Gaussian-process regression with subsequent optimization minimizing the objective function within 3.1% of those those obtained using the full model representation, but for 74% of the computational cost (far fewer model runs). This framework facilitates more efficient parameterization of the turbulence-source equations using turbine-wake data.

Word Count: 3728
Number of Tables: 6
Number of Figures: 3
Number of References: 50

Corresponding Author:
Sterling Olson
3408 Valencia Dr. NE, Albuquerque NM, 87110
(706) 339-9552
ssolson@sandia.gov

Acknowledgements:
The authors would like to thank Dr. Scott James and Baylor University for his assistance in the preparation of this article.
Sandia National Laboratories is a multimission laboratory managed and operated by National Technology & Engineering Solutions of Sandia, LLC, a wholly owned subsidiary of Honeywell International Inc., for the U.S. Department of Energy's National Nuclear Security Administration under contract DE-NA0003525. This paper describes objective technical results and analysis. Any subjective views or opinions that might be expressed in the paper do not necessarily represent the views of the U.S. Department of Energy or the United States Government.

*Cover Letter

Sterling Olson
3408 Valencia Dr. NE
Albuquerque, NM
USA
✉ *ssolson@sandia.gov*

Soteris Kalogirou
Renewable Energy,

February 5, 2019

Dr. Kalogirou,

We wish to submit an original research article entitled "*Turbulence-parameter Estimation for Current-energy Converters Using Surrogate Model Optimization*" by authors Sterling Olson (MS- Chemical Engineering), Dr. Jack C.P. Su (Ph.D Operations Management), Dr. Humberto Silva III (Ph.D Aerospace Engineering), Chris Chartrand (MS Mechanical Engineering), and Jesse Roberts (MS Mechanical Engineering) for consideration by Renewable Energy. This work grew out of work published in Renewable Energy by James et. al. (see article reference [16]), to determine the optimal tunable turbulent source term constants. The work pivoted to determine a more computationally efficient manner of tuning these constants using a surrogate model.

A wide variety of Renewable Energy readers will find this work interesting as it combines experimental, simulation, and machine learning techniques applied to marine renewable energy to develop a generalized procedure at lower computational costs. The procedure developed here may be applied by researchers using environmental tools to tune an actuator disc power generation method to laboratory scale experiment for marine current energy converters in mesoscale applications. In additionally to growing out of work previously published in Renewable Energy this manuscript references 7 articles published in Renewable Energy.

Each of the authors confirms that this manuscript has not been previously published and is not currently under consideration by any other journal. This work will be applied to a Thesis defense following appropriate steps to expand the work and ensure the work is sufficiently different. Additionally, all of the authors have approved the contents of this paper and have agreed to the Renewable Energy's submission policies. All authors have approved the manuscript and agree with its submission to Renewable Energy.

Should you select our manuscript for peer review, we would like to suggest the following potential reviewers/referees because they would have the requisite background to evaluate our findings and interpretation objectively.

- Dr. Craig Jones, Integral Consulting (cjones@integral-corp.com)
- Dr. Daniel Apellö, University of Colorado Boulder (Daniel.Appelo@Colorado.edu)
- Mr. Carlos Ströfer, Virginia Polytechnic Institute and State University (cmich@vt.edu)

To the best of our knowledge, the above-suggested persons do not have any conflict of interest, financial or otherwise. Dr. Scott James whose research this builds upon was not recommended because he was a paid consultant for the work.

Each of the authors confirms that this manuscript has not been previously published and is not currently under consideration by any other journal. This work will be applied to a thesis defense following appropriate steps to expand the work and ensure the work is sufficiently different. Additionally, all of the authors have approved the contents of this paper and have

agreed to the Renewable Energy's submission policies. All authors have approved the manuscript and agree with its submission to Renewable Energy.

Thank you for your consideration,

Sterling Olson

*Highlights

Sterling Olson
3408 Valencia Dr. NE
Albuquerque, NM
USA

February 5, 2019

The highlights for this paper include:

- A surrogate model accurately predicted center-line wake recovery behind a marine turbine model
- Proposed a generalize surrogate model development and optimization procedure
- Surrogate model optimization result comparable to the full model result
- Surrogate model used only 74% computational cost compared to the full model optimization

Thank you for your consideration,

Sterling Olson

Turbulence-parameter Estimation for Current-energy Converters Using Surrogate Model Optimization

Sterling S. Olson[a,b,c], Jack C. P. Su[b], H. Silva III[c,d],
Chris C. Chartrand[a], Jesse D. Roberts[a]

[a]*Sandia National Laboratories, Water Power Technologies Department, Albuquerque, NM, USA*

[b]*The University of New Mexico, Anderson School of Management, Albuquerque, NM, USA*

[c]*The University of New Mexico, Department of Mechanical Engineering, Albuquerque, NM, USA*

[d]*Sandia National Laboratories, Thermal Sciences & Engineering, Albuquerque, NM, USA*

February 6, 2019

Abstract

Surrogate models maximize information utility by building predictive models in place of computational or experimentally expensive model runs. Marine hydrokinetic current energy converters require large-domain simulations to estimate array efficiencies and environmental impacts. Meso-scale models typically represent turbines as actuator discs that act as momentum sinks and sources of turbulence and its dissipation. An OpenFOAM model was developed where actuator-disc k-ϵ turbulence was characterized using an approach developed for flows through vegetative canopies. Turbine-wake data from laboratory flume experiments collected at two influent turbulence intensities were used to calibrate parameters in the turbulence-source terms in the k-ϵ equations. Parameter influences on longitudinal wake profiles were estimated using Gaussian-process regression with subsequent optimization minimizing the objective function within 3.1% of those those obtained using the full model representation, but for 74% of the computational cost (far fewer model runs). This framework facilitates more efficient parameterization

of the turbulence-source equations using turbine-wake data.

Keywords: Actuator disc, OpenFOAM, Gaussian-process regression, Surrogate; Turbulence

1 Introduction

Marine hydrokinetic (MHK) energy is an appealing domestic, renewable resource. Unlike many renewables, tides are predictable and resources are often close to population centers. Technology developers must reduce the time and costs to meet regulatory requirements especially with regard to the potential environmental impacts associated with deploying arrays of MHK devices. Research at Sandia National Laboratories (SNL) and elsewhere has demonstrated that a small number of devices does not cause environmental concern [50]. However, commercial-scale deployments must be analyzed to ensure environmental tipping points are not exceeded. As MHK-driven changes to the flow environment may affect the local ecosystem and aquatic life, tools that facilitate the virtual design of array layouts must be developed and validated to simulate flows through and around MHK arrays and then estimate environmental responses [32].

As MHK arrays may occupy tens to hundreds of square kilometers, supercomputers are required for high-spatial-resolution, spinning-turbine simulations [7, 8, 18]. However, reduced-order models (e. g., representing turbines by actuator discs and solving for flow fields using the shallow-water equations) are typically implemented to facilitate timely decision making. Turbines can be analytically and numerically approximated with actuator discs, which although they do not rotate, they remove momentum from the system by converting it into turbulent kinetic energy [2]. Borrowing upon research from the wind-energy community [40, 41], k-ϵ turbulence-source terms originally developed for wind transport through vegetative canopies [19, 37] have been incorporated into the environmental

flow codes SNL-Delft3D-CEC [44] and SNL-EFDC [16].

Developing simulation tools for wave and tidal devices has been identified as a top priority for bringing marine renewable energy to market [1, 47]. Data and computational needs have motivated laboratory-scale experiments, which help reduce capital expenditures associated with sea deployments [23, 28, 29, 30, 33, 45]. Data from laboratory flume experiments have been used to calibrate numerical models including blade and blade-design models [26, 22], electrical-performance models [12], blade element method (BEM) models [24], actuator-disc models [14], and turbulence models [16]. However Gaurier et al. [13] questions experimental standards and design while Neary et al.[31] raises concerns about the use of common measurement tools in laboratory and field experiments both of which complicate comparisons between data sets and model calibration efforts. Here, the authors focus on one experimenters data set collected at two influent turbulent intensities (I_∞) [28].

2 Motivation

A computational fluid dynamics OpenFOAM [46] model was used to simulate the wake behind a scaled turbine placed in an experimental flume. The four adjustable parameters governing the source terms in the canopy k-ϵ model [40] were calibrated to match experimental quantities of interest (QoIs), specifically longitudinal profiles of velocity, U, and turbulence intensity, I [28]. Given the computational expense of this process, a more efficient framework was developed where adjustable parameters were preselected and Gaussian process regression (GPR) [4] was used to predict longitudinal QoI profiles. After GPR development, its predictions yielded nearly instantaneous results compared to running the CFD simulation. Optimizing the turbulence parameters with GPR can significantly accelerate the calibration process. Here, we define a GPR surrogate model [39] as a data-driven technique to empirically approximate the response surface of a physics-based model. These have alternately been called "metamodels" [5, 20], "model emulators" [34], and "proxy models"

[3].

3 Framework Development

3.1 Flume Experiment

Mycek et al. [28] studied a three-bladed horizontal-axis turbine with diameter $d_t = 0.7\,\text{m}$ in the IFREMER flume in France. The 18 m-long, 4 m-wide flume conveyed 2 m-deep water at an average velocities of $U_\infty = 0.8\,\text{m/s}$, each at two influent I_∞ $I_{3\%}$ and $I_{15\%}$. The turbine blockage ratio was 4.81%. At $U_\infty = 0.8\,\text{m/s}$, measured thrust coefficients were $C_t = 0.8$ and 0.72 at $I_{3\%}$ and $I_{15\%}$, respectively. Wake recovery was characterized by U and TI measured at 10 longitudinal locations downstream of the turbine: namely $x^* = 1.2, 2, 3, 4, 5, 6, 7, 8, 9, 10$ where $x^* = x/d_t$. The horizontal distribution of the wake was characterized at 26 points measured laterally at each of the 10 downstream locations. This calibration effort considered only the experimental results where $U_\infty = 0.8\,\text{m/s}$ for both $I_{3\%}$ and $I_{15\%}$. Lateral profiles were not included in this initial investigation due to asymmetry in the lateral profiles and because the focus was on determining if the surrogate model could perform well for a representative subset of the data to determine proof of concept.

3.2 OpenFOAM Model Development

Open-source OpenFOAM v5.0 was used to develop a CFD model of the IFREMER flume experiment. The InterFOAM solver specified the flow field using the Reynolds-averaged Navier-Stokes (RANS) two-phase volume of fluid (VOF) technique with the k-ϵ turbulence model [21]. Figure 1 shows the OpenFOAM model domain simulated with a symmetry plane along the flow direction to reduce computational expense (width was 2 m). The symmetry plane bisected the 0.1 m-thick actuator disc located $x = 6\,\text{m}$ from the inlet. Inlet flow was specified uniformly as $U_\infty = 0.8\,\text{m/s}$. The influent turbulence values were specified as for k and ϵ as $k = 3/2(I_\infty U_\infty)^2$ and $\epsilon = c_\mu * k^{3/2}/d_t$. At the outlet,

pressure was maintained 2 m above the flume floor with 0.5 m of air above the water. As vertical velocity profiles were not measured and boundary-layer theory for flow over a flat plate suggests that the boundary layer was only ~ 0.1 m tall, free-slip conditions were applied along the flume floor and walls. The elevation of the free surface was internally calculated by the VOF technique, but was constrained by the specified-pressure outlet boundary condition. The OpenFOAM model was run using mixed-order solution techniques including 1^{st} order for k and ϵ (upwind) and 2^{nd} order for U divergence (linear upwind). The observed orders of convergence for U and k were to be 2.08 and 1.94 respectively for the $I_\infty = 3\%$ case at x^*5.

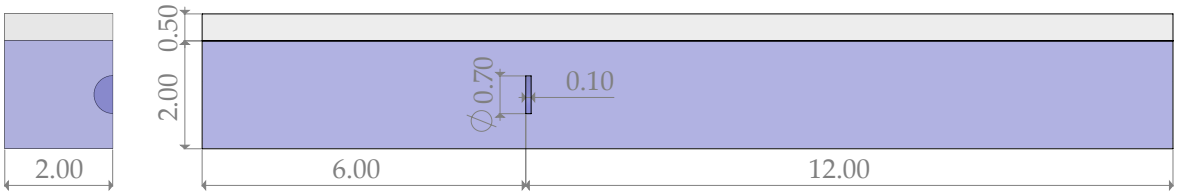

Figure 1: Model domain dimensions [m] for the front (left) and side (right) view along the symmetry plane.

3.3 Turbulence-source Equations

k-ϵ turbulence-equation source terms were developed to simulate turbulent flows through vegetative canopies [19, 37] and have since been applied to wind turbines [40, 41] and MHK models [16]. Sources of turbulent kinetic energy, k (m^2/s^2), and its dissipation rate, ϵ (m^2/m^3), are:

$$S_k = \frac{1}{2} C_x \left(\beta_\mathrm{p} U^3 - \beta_\mathrm{d} U k \right), \tag{1}$$

$$S_\epsilon = \frac{1}{2} C_x \left(\beta_\mathrm{p} C_{\epsilon 4} \frac{\epsilon}{k} U^3 - \beta_\mathrm{d} C_{\epsilon 5} U \epsilon \right), \tag{2}$$

where C_x (–) is the modified thrust coefficient, and U (m/s) is the velocity at the turbine/actuator disc. Adjustable parameter β_p (–) is the fraction of k converted to wake-generated kinetic energy by drag, which accounts for the production of wake turbulence and represents the ratio of mean

kinetic energy transferred directly into turbulence (not the shear-generated turbulence). Adjustable parameter β_d (–) accounts for k dissipation through conversion to kinetic energy by the turbine blades (or actuator disc), or the short-circuiting of the turbulence cascade where energy transfers from large-scale turbulence to smaller scales. Adjustable parameters $C_{\epsilon 4}$ and $C_{\epsilon 5}$ are closure constants [48]. For vegetative canopies, Katul et al. [19] suggested $\beta_\mathrm{p} = 1$, $\beta_\mathrm{d} = 5.1$, $C_{\epsilon 4} = 0.9$, and $C_{\epsilon 5} = 0.9$, for wind turbines Réthoré et al. [41] suggested $\beta_\mathrm{p} = 0.05$, $\beta_\mathrm{d} = 1.6$, $C_{\epsilon 4} = 1.5$, and $C_{\epsilon 5} = 0.2$, and for actuator discs representing current energy converters (CECs) James et al. [16] suggested $\beta_\mathrm{p} = 0.96$, $\beta_\mathrm{d} = 1.38$, and $\beta_\mathrm{p} C_{\epsilon 4} = \beta_\mathrm{d} C_{\epsilon 5} = 3.87$.

Equations (1) and (2) depend on U, but the presence of the device alters the local flow field so the device-specific thrust coefficient, C_t (–) must be amended as [43]:

$$C_\mathrm{d} = 2\frac{1-\sqrt{1-C_\mathrm{t}}}{1+\sqrt{1-C_\mathrm{t}}}, \tag{3}$$

$$C_x = \rho A_\mathrm{d} C_\mathrm{d}, \tag{4}$$

where A_d (m^2) is the flow-facing area of the actuator disc and ρ ($\mathrm{kg}/(\mathrm{m}^3)$ is the water density.

3.4 Metrics

The three metrics defined in Table 1 were used to compare the QoIs (Q) between the experimental measurements (exp), OpenFOAM simulations, (sim), and surrogate-model estimates (srgt). Given that the two QoIs (U, I), at two I_∞ (3%, 15%) are sampled at 10 points in the wake, there were a total of $N = 40$ values for a total model comparison, and $N = 10$ for any QoI at a given I_∞.

All metrics listed in Table 1 are provided at each appropriate step, however specific metrics defined here are used for surrogate model decision making. The fitting error compares the predictions of the surrogate model and the simulation. Fitting error determines if the developed surrogate model is of sufficient accuracy to proceed to optimization and if the surrogate model represents the CFD simulator well at the final value obtained by optimization. The predicted error is minimized during

Table 1: Performance metrics.

Comparisons	Mean absolute percentage error (MAPE)	Mean squared error (MSE)	Maximum error ($\lvert L_\infty \rvert$)
sim/exp	$\frac{100}{N}\sum_{i=1}^{N}\left\lvert\frac{Q_{\text{sim}}-Q_{\text{exp}}}{Q_{\text{exp}}}\right\rvert_i$	$\frac{1}{N}\sum_{i=1}^{N}\left(\frac{Q_{\text{sim}}-Q_{\text{exp}}}{Q_{\text{exp}}}\right)_i^2$	$100\cdot\max\left\lvert\frac{Q_{\text{sim}}-Q_{\text{exp}}}{Q_{\text{exp}}}\right\rvert_i$
srgt/sim	$\frac{100}{N}\sum_{i=1}^{N}\left\lvert\frac{Q_{\text{srgt}}-Q_{\text{sim}}}{Q_{\text{sim}}}\right\rvert_i$	$\frac{1}{N}\sum_{i=1}^{N}\left(\frac{Q_{\text{srgt}}-Q_{\text{sim}}}{Q_{\text{sim}}}\right)_i^2$	$100\cdot\max\left\lvert\frac{Q_{\text{srgt}}-Q_{\text{sim}}}{Q_{\text{sim}}}\right\rvert_i$
srgt/exp	–	$\frac{1}{N}\sum_{i=1}^{N}\left(\frac{Q_{\text{srgt}}-Q_{\text{exp}}}{Q_{\text{exp}}}\right)_i^2$	–

optimization and is equivalently the objective function for the surrogate model optimization. As an optimization of the full CFD and the surrogate is provided in this work, the predicted error term allows for simple reference to refer to the surrogate model optimization. Lastly, final error refers to the optimization values which minimize predicted error, run in the full CFD simulator (OpenFOAM) compared to the physical experiment. The term final error is used as it represents the ultimate goal of the surrogate model optimization. The use of these terms in relation to the overall surrogate model development is formally defined in Section 4.5: Surrogate Model Optimization Framework.

Fitting Error Indicates the difference between surrogate model predictions and simulation prediction by $MAPE_{srgt/sim}$

Predicted Error The difference between surrogate model prediction and physical experiment by $MSE_{srgt/exp}$

Final Error At optimal setting, the difference between simulation result and physical experiment by $MSE_{sim/exp}$

3.5 k-ϵ Model Results

Prior to tuning the standard k-ϵ model was run without turbulent sources sources (Equivalently $0 = \beta_p = \beta_d = C_{\epsilon 4} = C_{\epsilon 5}$) to demonstrate the necessity and impact of the source terms and quantify model error corrected by the canopy k-ϵ model. Using the metrics described in Table 1 the model errors listed in Table 2 were highest when turbulence was lowest ($I_{3\%}$) for all but $|L_\infty|$ at $I_{15\%}$. The average model error when compared to experiment was 28.2% by MAPE and around 20% for for each QoI except $U_{3\%}$ where the wake recovery was predicted to be significantly faster than experiment. Through tuning the turbulent sources the model error compared to experiment will be significantly reduced.

Table 2: Model errors without k-ϵ sources.

QoI	$\text{MAPE}_{\text{sim/exp}}$	$\text{MSE}_{\text{sim/exp}}$	$\lvert L_\infty \rvert_{\text{sim/exp}}$
$U_{3\%}$	50.3%	11.5	77.3%
$U_{15\%}$	21.3%	4.5	82.4%
$I_{3\%}$	23.3%	2.8	39.6%
$I_{15\%}$	18.0%	2.3	45.7%
Mean	28.2%	21.1	61.3%

3.6 PEST Calibration/Parameter Estimation

Model error to experiment was improved through the calibration of the turbulent source terms. Calibration was performed using the model-independent, Parameter ESTimation (PEST) software suite [9]. PEST was supplied with four adjustable parameters (β_p, β_d, $C_{\epsilon 4}$, $C_{\epsilon 5}$) and 40 experimental observations (10 measurements downstream of the turbine for each QoI) to formulate the objective function as:

$$\text{MSE} = \frac{1}{N}\sum_{i=1}^{N} w_i \left(\frac{Q_\text{predicted} - Q_\text{exp}}{Q_\text{exp}} \right)_i^2, \tag{5}$$

where i is a measured observation, N is the total number of observations, w_i is the weight assigned to each observation, and $Q_{\text{predicted}}$ and Q_{exp} are the OpenFOAM equivalents to the experimental QoIs (turbulence intensity and velocity along the centerline of the wake), respectively. Unit weights were applied to all observations. Moreover, U and TI were normalized to each range from 0 to 1.

PEST was applied to both the OpenFOAM and GPR surrogate models. Parameters β_{p} and β_{d} were initially specified according to the results from James et al. [16]. Due to the use of a different turbulence model, initial guesses of 0.9 were used for $C_{\epsilon 4}$ and $C_{\epsilon 5}$ as suggested by Katul et al. [19]. All lower bounds were set to 0.1. For surrogate model construction, the sampled space must be representative, but the broader the parameter range, the more sample points required to develop the GPR. The upper bound of β_{p} is physically limited to 1 because this is the fraction of kinetic energy converted to k. The upper bound of β_{d} was set to 4. The upper bounds of $C_{\epsilon 4}$ and $C_{\epsilon 5}$ were commensurately set equal to 1 and 4, respectively. These ranges were sufficient to afford comparisons between OpenFOAM model optimizations and GPR model optimization.

4 Surrogate Model Development

For models with long run times exceeding 24 hours, calibration becomes intractable because in addition to the many required model calls, the calibration process itself is iterative; rarely is an acceptable calibration achieved on the first try. Alternately, pre-sampling parameter space and building a GPR surrogate model can speed up the process if the surrogate model sufficiently approximates the computationally expensive model [10]. Nevertheless, care must be taken when constructing the surrogate model to ensure that it is a valid substitute for the full, physics-based model.

4.1 Gaussian Process Regression

A Gaussian process is a subset of a stochastic process where an n dimensional real input vector $\mathbf{x}$ and any finite number of determined random variables are specified to have a joint Gaussian distribution. A Gaussian process defines a prior distribution over functions which when supplied data may be used to define a posterior distribution over functions [42]. Here the distribution over functions is accomplished by using the one-to-one mapping between input $\mathbf{x}$ and output $f(\mathbf{x})$ to describe the functional output as normally distributed and this may be defined as a Gaussian process i.e. $f(\mathbf{x}) \sim \mathcal{N}(\mu, \sigma^2 I) \Rightarrow f(\mathbf{x}) \sim GP(m(\mathbf{x}), k(\mathbf{x}, \mathbf{x}'))$ (See Rasmussen et al. [38]). The Gaussian process is fully specified by the mean function $m(\mathbf{x})$ and covariance function $k(\mathbf{x}, \mathbf{x}')$ where $\mathbf{x}$, $\mathbf{x}'$ is any point in the input domain $\mathbf{x}$. The covariance function or kernel may take many forms such that the kernel is semi-positive definite and has the property that as $x - x' \to \infty$, $k(x, x') \to 0$; as the distance between any two points increases, the covariance between those two points tends to zero. GPR is considered local because predictions are weighted averages of measurements in the neighborhood of the point where the system is estimated [36]. For this work a radial basis function (Equation 6) with hyperparameters α, ℓ, and σ was selected as the kernel:

$$k(x, x') = \sigma^2 \left[1 + \frac{(x - x')^2}{2\alpha\ell^2}\right]^{-\alpha}, \tag{6}$$

where σ^2 is the kernel scale factor, α is the inverse variance parameters, and ℓ is the length scale defined as the distance between x and x' where the covariance can be considered zero. Similar to variance, the scale factor describes the average squared distance of the kernel function from its mean. Hyperparameter α characterizes the "smoothness" of the function where increasing α leads to smoother responses. Hyperparameters, α, ℓ, and σ, were specified through an optimization process that maximized the log-marginal likelihood defined as.

$$\mathcal{H} = \log p\left(y_i|x_i,\Theta\right) = -\frac{1}{2}\log\left|k(x,x')\right| - \frac{1}{2}\left(y_i-\mu\right)^{\top} k\left(x,x'\right)^{-1}\left(y_i\right) - \frac{n}{2}\log\left(2\pi\right), \tag{7}$$

where y_i is a vector of observed target values (QoIs), the mean function μ is assumed zero, n is the number of components in x_i and Θ represents the hyperparameters in the kernel function. For the optimization, hyperparameter bounds were specified as $\sigma^2 \in [0.1, 10]$, $\alpha \in [10^{-4}, 2]$, and $\ell \in [0.1, 2]$. As suitable hyperparameters values were not known prior to data fitting bounds for σ^2 and α were adjusted such that the bound were not reached during the hyper parameters optimization. However, ℓ was limited to 2 to prevent overfitting [27].

4.2 Surrogate Model Sample Space

Five-point sampling was performed across parameter bounds $\beta_{\mathrm{p}}, C_{\epsilon 4} \in [0.1, 1]$ and $\beta_{\mathrm{d}}, C_{\epsilon 5} \in [0.1, 4]$. Parameter lower limits were 0.1 because a zero value for one parameter of the pair obviates the effect of the other. The five points were $\beta_{\mathrm{p}}, C_{\epsilon 4} \in [\underline{0.1}, 0.325, \underline{0.55}, 0.775, \underline{1.0}]$ and $\beta_{\mathrm{d}}, C_{\epsilon 5} \in [\underline{0.1}, 1.075, \underline{2.05}, 3.025, \underline{4.0}]$ with underlined values used to construct the surrogate model resulting in 81 samples (3^4). Non-underlined values were used for verification totaling 16 samples (2^4). OpenFOAM was run using these 97 parameter samples to generate and validate the QoI response surface as a function of the adjustable parameters.

4.3 Building the Surrogate Model

Four GPR models, one for each QoI, were built because a single kernel function was found insufficient to determine a relationship for each QoI at each I_∞. The GPR surrogate models were constructed using Python version 2.7.12 with Numpy version 1.13.1. Data storage and handling were completed using Scipy 0.19.1 and Pandas version 0.20.3. The GPR itself was trained using Scikit-Learn 0.19.2. Plots were made using Matplotlib version 1.5.3. [15, 17, 25, 35].

For a single set of parameters $(\beta_{\mathrm{p}}, \beta_{\mathrm{d}}, C_{\epsilon 4}, C_{\epsilon 5})$ a "model call" required two OpenFOAM model runs (one each for the $I_{3\%}$ and $I_{15\%}$ boundary conditions). From each OpenFOAM model run, the simulated QoIs at the 10 points downstream of the turbine, yielded 810 data points to train each GPR model and 160 verification points. The GRP model was trained to maximize the log-marginal likelihood by adjusting the kernel hyperparameters using the SciPy optimization routine, `fmin_l_bfgs_b`, which is a quasi-Newton algorithm for constrained optimization [6, 17]. Five restarts (number of times an optimization was initiated using random hyperparameters) were specified; increases did not further improve the kernel optimizations shown in Table 3.

Table 3: Optimized hyperparameters.

QoI	σ	ℓ	α	Log-marginal likelihood
$U_{3\%}$	0.35	2.0	0.024	1,211
$U_{15\%}$	0.16	2.0	0.044	1,831
$I_{3\%}$	0.17	2.0	0.082	1,813
$I_{15\%}$	0.11	2.0	0.055	2,143

Most notably in Table 3 the ℓ all hit the maximum at 2.0, which is due to the tendency of GPR to overfit the data [27]. Not limiting ℓ resulted in $\ell = 4.8$, 10, 5.5, and 5.8 for $U_{3\%}$, $U_{15\%}$, $I_{3\%}$, and $I_{15\%}$, respectively, while only raising the log-marginal likelihood on the order of 2%. The small value of α suggest that the GPR are less smooth than a radial basis function while σ is reasonably consistent across the models.

4.4 Surrogate-model Performance

To verify that the surrogate model represented the OpenFOAM model, the 16 parameter sets excluded from GPR training were used for verification with results listed in Table 4. All $\mathrm{MAPE}_{\mathrm{srgt/sim}}$ results were $< 10\%$. The better performance of the $I_{15\%}$ is not guaranteed but potentially expected due to the higher log-marginal likelihood noted in Table 3.

Table 4: GPR OpenFOAM surrogate model performance as compared to true OpenFOAM model.

QoI	$\text{MAPE}_{\text{srgt/sim}}$	$\text{MSE}_{\text{srgt/sim}}$	$\lvert L_\infty \rvert_{\text{srgt/sim}}$
$U_{3\%}$	4.8%	0.7	14.9%
$U_{15\%}$	1.5%	0.2	9.7%
$I_{3\%}$	9.8%	17.8	49.7%
$I_{15\%}$	3.4%	3.5	21.1%
Mean	4.9%	5.5	23.9%

4.5 Surrogate Optimization Framework Development

Figure 2 shows the framework for building, verifying, and optimizing the surrogate model. After defining adjustable parameter space (Section 4.2), the GPR surrogate model was developed using data from OpenFOAM model runs. Once the GPR model fitting error was demonstrated to be <10% at the verification points, PEST was applied to the GPR model to minimize predicted error, now labeled GPR-PEST. Next, the GPR-PEST calibrated parameters were supplied to the OpenFOAM model to verify that fitting error at the optimized point was <10% on average. If not this process (build GPR and minimize predicted error) was repeated, iteratively updating the GPR model training data using the optimized point until the fitting error at the optimized point was <10% on average. Finally, the GPR-PEST parameters were evaluated in OpenFOAM simulations according to the three performance metrics listed in Table 1 and the final error was reported.

5 Results and Discussion

5.1 Surrogate and OpenFOAM Parameter Estimates

The optimized parameter values for the GPR-PEST and OpenFOAM-PEST are organized in Table 5. The GPR column has two final results as two surrogate model iteratons were required to achieve a complete optimization. The first GPR-PEST optimization (Final_1) minimized predicted error ($\text{MSE}_{\text{srgt/exp}}$) to 0.084 but the fitting error ($\text{MAPE}_{\text{srgt/sim}}$) was equal to 22.4% exceeding the 10%

Table 5: OpenFOAM and GPR-surrogate estimated parameters and corresponding performances.

	GPR		OpenFOAM
Parameter	Final_1	Final_2	Final
β_p	1.00	1.00	1.00
β_d	1.05	0.80	1.84
$C_{\epsilon 4}$	1.00	1.00	0.77
$C_{\epsilon 5}$	0.10	0.16	0.13
Predicted Error	0.084	0.043	–
Fitting Error	22.4%	3.6%	–
Final Error	–	0.0358	0.0347

acceptance criterion (Figure 2). Therefore, the OpenFOAM results from the Final_1 case (β_p, β_d, $C_{\epsilon 4}$, $C_{\epsilon 5}$ = 1.0, 1.05, 1.0, 0.1) were added to the original 81 OpenFOAM sample points and the GPR model was rebuilt now using 82 training points. A PEST optimization identical to the first was repeated on the new GPR surrogate model. This optimization (Final_2) decreased the predicted error to 0.043 with an acceptable fitting error of 3.6%. This concluded the GPR optimization with a total of 99 model calls (81 training, 16 verification, 2 final). The GPR-PEST final error ($\text{MSE}_{\text{sim/exp}}$) was 0.0358, lower than the GPR predicted error (0.043).

Success of the GPR-PEST optimization was determined by comparison to an equivalent optimization of the OpenFOAM simulation shown in the final column (OpenFOAM) of Table 5. While the OpenFOAM-PEST further minimized the final error (0.0347), the GPR-PEST achieve a result within 3.1% of the OpenFOAM-PEST result. GPR-PEST and OpenFOAM-PEST turbulence parameter values differed primarily for parameters β_d and $C_{\epsilon 4}$. OpenFOAM-PEST parameters plugged into the GPR model returned high predicted error and therefore without expanding the training data the GPR model would not achieve the same parameter solution as OpenFOAM-PEST. While definitive discussion of the turbulence parameter differences (β_d and $C_{\epsilon 4}$) cannot be made because k and ϵ are both coupled and nonlinear, the direction of the parameter changes makes sense following from Equations 1 and 2. It is possible that the GPR-PEST solution counterbalances the decrease of β_d

(increasing k) with the increase of $C_{\epsilon 4}$ (increasing ϵ / dissipation of k) which results in a nominally similar solution to the OpenFOAM-PEST solution.

Both the GPR-PEST and the OpenFOAM-PEST results suggest that $\beta_{\mathrm{p}} = 1.0$ which is the upper bound as the quantity represent the fraction of *tke* converted to wake-generated kinetic energy by drag. It is physically unreasonable to assume that all *tke* is converted to wake-generated kinetic energy by drag and may suggest that these turbulence source term solutions are currently accounting for more model form error than simply turbulence. Secondly the GPR hits the upper-bound of 1.0 for $C_{\epsilon 4}$. This ostensibly suggests that the GPR-PEST results may have further increased $C_{\epsilon 4}$ if permitted. The surrogate model training data necessary to extend a boundary would require 27 (3^3) additional model runs to provide identical information to the current training data boundary points, though the user may determine another method to keep the additional model call number down. However, for this case it can be seen that within the given range of turbulence parameters a lower object function value ($\mathrm{MSE}_{\mathrm{sim/exp}} = 0.0347$) existed as identified by the OpenFOAM-PEST results but was not identified by the GPR. This demonstrates both that extending the boundary using an additional 27 model calls may have not been the best use of expensive computational resources and the susceptibility of the GPR surrogate model to find local minima.

The GPR-PEST optimization minimized the final error within 3.1% of an equivalent OpenFOAM-PEST optimization. The parameters used in a gradient based search optimization tool such as PEST are often adjusted following an iterative procedure [49]. PEST results reported in Table 5 took many hundreds of PEST optimizations to achieve. To make the most objective comparison of the total number of model calls between the surrogate procedure and the OpenFOAM-PEST optimization a new PEST control file was created following the guidance of *Getting the Most of of PEST* [11]. This singular PEST run took a total of 134 model calls but returned a higher final error (0.0354) than the reported OpenFOAM-PEST results in Table 5. This PEST control file

would need to be iterativly adjusted to achieve final error as low as reported in Table 5 but serves as a fair comparison for the total number of model calls. The GPR-PEST model used a total of 99 equivalent model calls thereby only enacting 74% of the computational expense of this singular OpenFOAM-PEST optimization (134 model calls). This decrease in model calls and the ability to utilize all information from expensive computations makes surrogate models of practical interest to researchers and practitioners alike.

5.2 Surrogate & OpenFOAM Parameter Values Compared to Experiment

Final error for the GPR-PEST and OpenFOAM-PEST are broken down in Table 6 for each QoI. The final error reported in Table 5 can be seen in in the "Mean" row under the $\text{MES}_{\text{sim/exp}}$ column. In each case the primary contributor to $\text{MSE}_{\text{sim/exp}}$ is $I_{3\%}$ due to a second increase in the experimentally measured I starting as four-diameters downstream as detailed in Mycek et al. [28]. Here it was not expected that the k-ϵ turbulence model could capture the delayed shear layer mixing caused by the low ambient turbulence ($I_\infty = 3\%$). In turbine deployment conditions an ambient turbulence of 3% is unlikely but tuning the turbulence model to this condition provides confidence as a good model should be valid over a large range of turbulence values. It can further be seen in each case the the least contributor to $\text{MSE}_{\text{sim/exp}}$ is $I_\infty = 15\%$ for both U and I. This is encouraging because I_∞ near 15% is typical in environmental applications.

Comparing GPR-PEST and OpenFOAM-PEST by $\text{MAPE}_{\text{sim/exp}}$ the average model fitness was 14.5% and 13.6% respectively. It may also be noted that the average maximum error ($|L_\infty|$) nominally equivalent between the two cases.

Figure 3 compares data (red dots) to OpenFOAM simulations using GPR-PEST (dashed curve) and OpenFOAM-PEST (solid curve) turbulence parameters. Further the standard k-ϵ actuator disc results (Table 2) are presented for reference (blue dash-dot curve). Optimized results were comparable

Table 6: Errors in simulated QoIs using optimized parameters from the GPR-PEST and OpenFOAM-PEST calibrations.

	GPR			OpenFOAM		
QoI	$\text{MAPE}_{\text{sim/exp}}$	$\text{MSE}_{\text{sim/exp}}$	$\lvert L_\infty \rvert_{\text{sim/exp}}$	$\text{MAPE}_{\text{sim/exp}}$	$\text{MSE}_{\text{sim/exp}}$	$\lvert L_\infty \rvert_{\text{sim/exp}}$
$U_{3\%}$	11.8%	0.0185	21.6%	11.9%	0.0193	22.1%
$U_{15\%}$	9.5%	0.0227	38.6%	8.8%	0.0256	41.2%
$I_{3\%}$	28.2%	0.0917	44.1%	27.1%	0.0880	43.7%
$I_{15\%}$	8.5%	0.0102	16.2%	6.4%	0.0058	11.5%
Mean	14.5%	0.0358	30.1%	13.6%	0.0347	30.2%

as noted in Table 6, but neither matched the experimental data (except for $I_{15\%}$) indicating model structural error. For each of the quantitative metrics in Table 6 the primary contributor to error for the QoI U was the near field velocity where correct representation using an actuator disc is a known issue. Further the plots definitively show the k-ϵ turbulence model's inability to represent the second bump in I at $I_\infty = 3\%$.

6 Conclusions

As industry develops MHK power, licensing will require environmental impact studies to demonstrate minimal environmental impacts. Calibrating actuator-disc models to experimental data is a necessary step to build confidence that the model will estimate environmental effects. A GPR surrogate of an OpenFOAM model was developed to decrease the computational expense of calibrating the parameters in the turbulence-source equations. Using GPR-PEST optimized turbulence parameters final error was within 3.1% of equivalently tuned OpenFOAM-PEST turbulence parameters for only 74% of the computational costs. The success of the surrogate model in this application demonstrates the ability to utilize all computationally expensive model calls for this domain specific calibration effort. Further, the success of a relatively simple surrogate model suggests that advanced surrogate

models investigations are worthy of future research.

7 Acknowledgements

Sandia National Laboratories is a multimission laboratory managed and operated by National Technology & Engineering Solutions of Sandia, LLC, a wholly owned subsidiary of Honeywell International Inc., for the U.S. Department of Energy's National Nuclear Security Administration under contract DE-NA0003525. This paper describes objective technical results and analysis. Any subjective views or opinions that might be expressed in the paper do not necessarily represent the views of the U.S. Department of Energy or the United States Government.

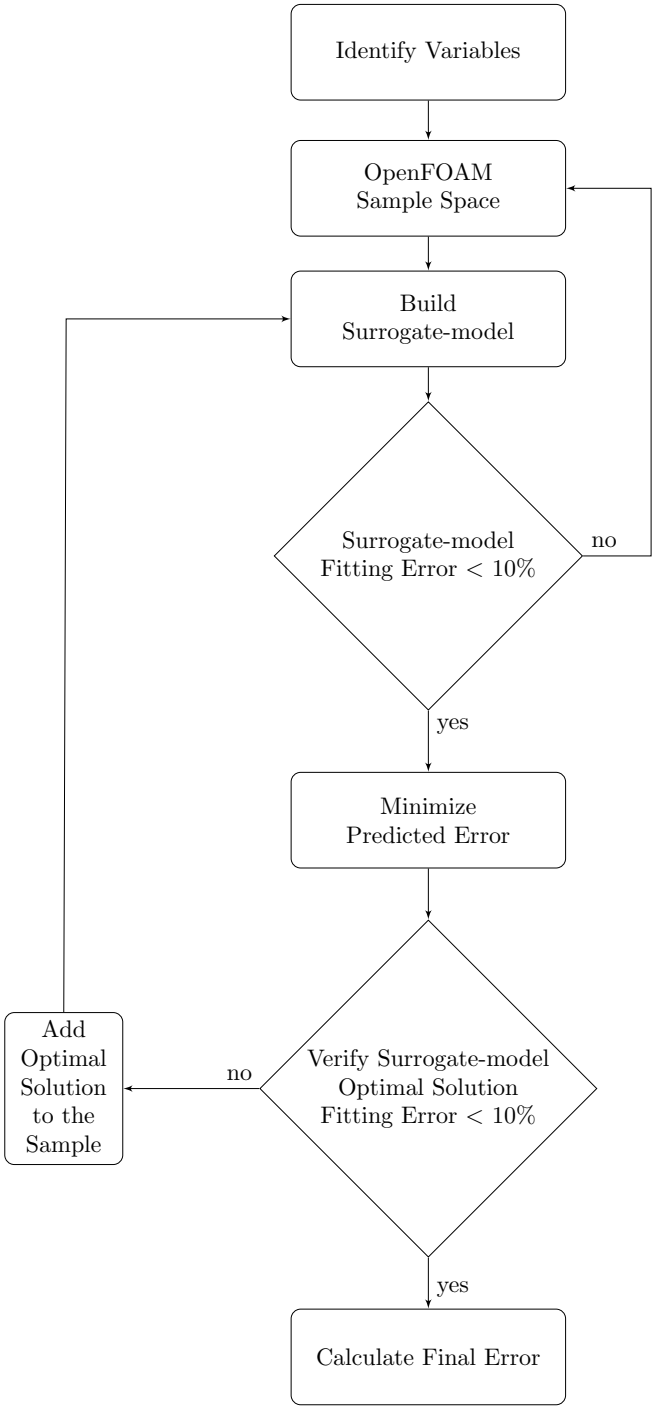

Figure 2: Flow diagram for the surrogate-model framework.

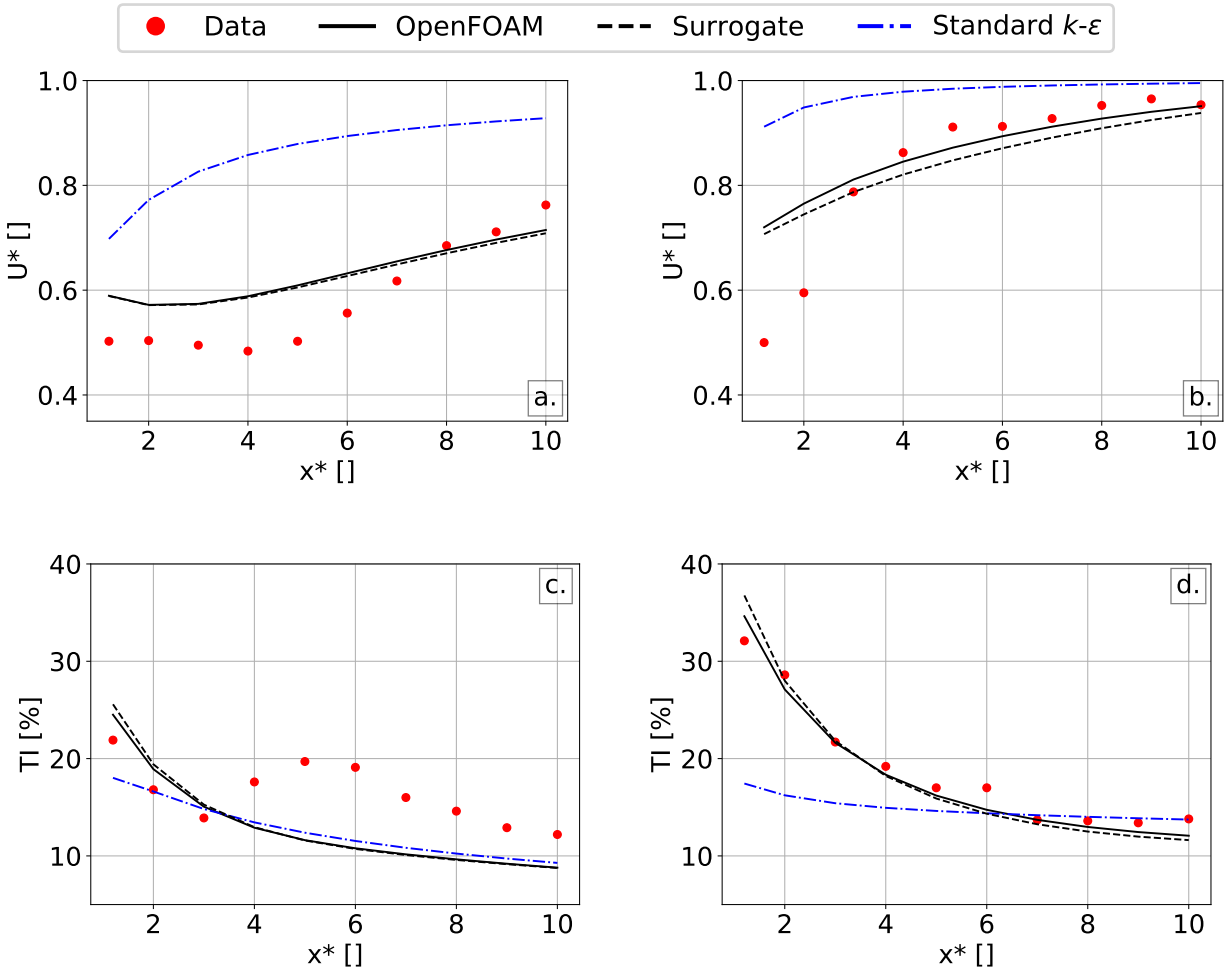

Figure 3: Comparison of experimental data (red dots) to optimized results using OpenFOAM (solid curve) and GPR (black-dashed curve) for QoIs U^* at (a) $I_{3\%}$ and (b) $I_{15\%}$ and I at (c) $I_{3\%}$ and (d) $I_{15\%}$. The standard k-ϵ actuator disc results are presented for reference (blue dash-dot curve).

References

[1] Bahaj, A., and Myers, L. E. Fundamentals applicable to the utilisation of marine current turbines for energy production. *Renewable energy 28*, 14 (2003), 2205–2211.

[2] Batten, W. M., Harrison, M., and Bahaj, A. Accuracy of the actuator disc-RANS approach for predicting the performance and wake of tidal turbines. *Phil. Trans. R. Soc. A 371*, 1985 (2013), 20120293.

[3] Bieker, H. P., Slupphaug, O., and Johansen, T. A. Real-time production optimization of oil and gas production systems: A technology survey. *SPE Production & Operations 22*, 4 (2007), 382–391.

[4] Bishop, C. M. *Pattern Recognition and Machine Learning (Information Science and Statistics)*. Springer, 2007.

[5] Blanning, R. W. The construction and implementation of metamodels. *SIMULATION 24*, 6 (1975), 177–184.

[6] Byrd, R. H., Lu, P., Nocedal, J., and Zhu, C. A limited memory algorithm for bound constrained optimization. *SIAM Journal on Scientific Computing 16*, 5 (1995), 1190–1208.

[7] Chamorro, L. P., Lee, S.-J., Olsen, D., Milliren, C., Marr, J., Arndt, R., and Sotiropoulos, F. Turbulence effects on a full-scale 2.5 MW horizontal-axis wind turbine under neutrally stratified conditions. *Wind Energy 18*, 2 (2015), 339–349.

[8] Chamorro, L. P., Troolin, D. R., Lee, S.-J., Arndt, R., and Sotiropoulos, F. Three-dimensional flow visualization in the wake of a miniature axial-flow hydrokinetic turbine. *Experiments in Fluids 54*, 2 (2013), 1459.

[9] Doherty, J. Model-independent Parameter Estimation User Manual Part I: PEST, SENSAN and Global Optimisers. *Watermark Numerical Computing* (2016), pp. 390.

[10] Doherty, J., and Christensen, S. Use of paired simple and complex models to reduce predictive bias and quantify uncertainty. *Water Resources Research 47*, 12 (2011).

[11] Doherty, John. Getting the Most out of PEST. http://www.pesthomepage.org/getfiles.php?file=pest_settings.pdf, 2013.

[12] Elghali, S. E. B., Balme, R., Le Saux, K., Benbouzid, M. E. H., Charpentier, J. F., and Hauville, F. A simulation model for the evaluation of the electrical power potential harnessed by a marine current turbine. *IEEE Journal of Oceanic Engineering 32*, 4 (2007), 786–797.

[13] Gaurier, B., Germain, G., Facq, J.-V., Johnstone, C., Grant, A., Day, A., Nixon, E., Di Felice, F., and Costanzo, M. Tidal energy "Round Robin" tests comparisons between towing tank and circulating tank results. *International Journal of Marine Energy 12* (2015), 87–109.

[14] Harrison, M., Batten, W., Myers, L., and Bahaj, A. Comparison between CFD simulations and experiments for predicting the far wake of horizontal axis tidal turbines. *IET Renewable Power Generation 4*, 6 (2010), 613–627.

[15] Hunter, J. D. Matplotlib: A 2D graphics environment. *Computing in Science & Engineering 9*, 3 (2007), 90–95.

[16] James, S. C., Johnson, E. L., Barco, J., and Roberts, J. D. Simulating current-energy converters: SNL-EFDC model development, verification, and parameter estimation. *Renewable Energy* (2017).

[17] Jones, E., Oliphant, T., Peterson, P., et al. SciPy: Open source scientific tools for Python, 2001–. [Online; accessed 11/17/2017].

[18] Kang, S., Borazjani, I., Colby, J. A., and Sotiropoulos, F. Numerical simulation of 3D flow past a real-life marine hydrokinetic turbine. *Advances in Water Resources 39* (2012), 33–43.

[19] Katul, G. G., Mahrt, L., Poggi, D., and Sanz, C. One-and two-equation models for canopy turbulence. *Boundary-Layer Meteorology 113*, 1 (2004), 81–109.

[20] Kleijnen, J. P. Kriging metamodeling in simulation: A review. *European Journal of Operational Research 192*, 3 (2009), 707–716.

[21] Launder, B. E., and Spalding, D. B. The numerical computation of turbulent flows. In *Numerical Prediction of Flow, Heat Transfer, Turbulence and Combustion*. Elsevier, 1983, pp. 96–116.

[22] Lee, J. H., Park, S., Kim, D. H., Rhee, S. H., and Kim, M.-C. Computational methods for performance analysis of horizontal axis tidal stream turbines. *Applied Energy 98* (2012), 512–523.

[23] Maganga, F., Germain, G., King, J., Pinon, G., and Rivoalen, E. Experimental characterisation of flow effects on marine current turbine behaviour and on its wake properties. *IET Renewable Power Generation 4*, 6 (2010), 498–509.

[24] Malki, R., Williams, A., Croft, T., Togneri, M., and Masters, I. A coupled blade element momentum–computational fluid dynamics model for evaluating tidal stream turbine performance. *Applied Mathematical Modelling 37*, 5 (2013), 3006–3020.

[25] McKinney, W. Data structures for statistical computing in python. In *Proceedings of the 9th Python in Science Conference* (2010), S. van der Walt and J. Millman, Eds., pp. 51–56.

[26] Michelen, C., Murray, J. C., Neary, V. S., Barone, M., et al. CACTUS open-source code for hydrokinetic turbine design and analysis: Model performance evaluation and public dissemination as open source design tool. Tech. rep., Sandia National Laboratories, 2014.

[27] Mohammed, R. O., and Cawley, G. C. Over-fitting in model selection with gaussian process regression. In *International Conference on Machine Learning and Data Mining in Pattern Recognition* (2017), Springer, pp. 192–205.

[28] Mycek, P., Gaurier, B., Germain, G., Pinon, G., and Rivoalen, E. Experimental study of the turbulence intensity effects on marine current turbines behaviour. Part I: One single turbine. *Renewable Energy 66* (2014), 729–746.

[29] Myers, L., and Bahaj, A. Experimental analysis of the flow field around horizontal axis tidal turbines by use of scale mesh disk rotor simulators. *Ocean Engineering 37*, 2-3 (2010), 218–227.

[30] Myers, L., and Bahaj, A. An experimental investigation simulating flow effects in first generation marine current energy converter arrays. *Renewable Energy 37*, 1 (2012), 28–36.

[31] Neary, V. S., Gunawan, B., Hill, C., and Chamorro, L. P. Near and far field flow disturbances induced by model hydrokinetic turbine: ADV and ADP comparison. *Renewable Energy 60* (2013), 1–6.

[32] Nelson, K., James, S. C., Roberts, J. D., and Jones, C. A framework for determining improved placement of current energy converters subject to environmental constraints. *International Journal of Sustainable Energy 37*, 7 (2018), 654–668.

[33] O'Doherty, T., Mason-Jones, A., O'Doherty, D., Byrne, C., Owen, I., and Wang, Y. Experimental and computational analysis of a model horizontal axis tidal turbine. In *8th European Wave and Tidal Energy Conference (EWTEC)* (Uppsala, Sweden, 2009).

[34] O'Hagan, A. Bayesian analysis of computer code outputs: A tutorial. *Reliability Engineering & System Safety 91*, 10 (2006), 1290–1300.

[35] Pedregosa, F., Varoquaux, G., Gramfort, A., Michel, V., Thirion, B., Grisel, O., Blondel, M., Prettenhofer, P., Weiss, R., Dubourg, V., Vanderplas, J., Passos, A., Cournapeau, D., Brucher, M., Perrot, M., and Duchesnay, E. Scikit-learn: Machine learning in Python. *Journal of Machine Learning Research 12* (2011), 2825–2830.

[36] Perner, P. *Machine Learning and Data Mining in Pattern Recognition: 9th International Conference, MLDM 2013, New York, NY, USA, July 19-25, 2013, Proceedings*, vol. 7988. Springer, 2013.

[37] Poggi, D., Porporato, A., Ridolfi, L., Albertson, J., and Katul, G. The effect of vegetation density on canopy sub-layer turbulence. *Boundary-Layer Meteorology 111*, 3 (2004), 565–587.

[38] Rasmussen, C. Cki williams gaussian processes for machine learning mit press. *Cambridge, MA* (2006).

[39] Razavi, S., Tolson, B. A., and Burn, D. H. Review of surrogate modeling in water resources. *Water Resources Research 48*, 7 (2012), W07401.

[40] Réthoré, P.-E., Sørensen, N. N., Bechmann, A., and Zhale, F. Study of the atmospheric wake turbulence of a cfd actuator disc model. In *European Wind Energy Convention* (2009), pp. 1–9.

[41] Réthoré, P.-E. M. *Wind turbine wake in atmospheric turbulence*. PhD thesis, Risø National Laboratory for Sustainable Energy, 2009.

[42] Robert, C. Machine learning, a probabilistic perspective, 2014.

[43] Roc, T., Conley, D. C., and Greaves, D. Methodology for tidal turbine representation in ocean circulation model. *Renewable Energy 51* (2013), 448–464.

[44] Sandia Energy. SNL-Delft3D-CEC. http://energy.sandia.gov/energy/renewable-energy/water-power/market-acceleration-deployment/snl-delft3d-cec/, 2017.

[45] Stallard, T., Collings, R., Feng, T., and Whelan, J. Interactions between tidal turbine wakes: Experimental study of a group of three-bladed rotors. *Phil. Trans. R. Soc. A 371*, 1985 (2013), 20120159.

[46] The OpenFOAM Foundation Ltd. OpenFOAM. https://openfoam.org/version/3-0-1/, 2017.

[47] Topper, M. B., and Ingram, D. M. Identifying the frontier of knowledge for marine renewable energy research. In *9th European Wave and Tidal Energy Conference* (2011).

[48] Warner, J. C., Sherwood, C. R., Arango, H. G., and Signell, R. P. Performance of four turbulence closure models implemented using a generic length scale method. *Ocean Modelling 8*, 1 (2005), 81 – 113.

[49] Watermark Numerical Computing. PEST Model-Independent Parameter Estimation User Manual Part I: PEST, SENSAN and Global Optimisers . http://www.pesthomepage.org/Downloads.php, 2016.

[50] Williamson, B. J., Blondel, P., Armstrong, E., Bell, P. S., Hall, C., Waggitt, J. J., and Scott, B. E. A self-contained subsea platform for acoustic monitoring of the environment around marine renewable energy devices–field deployments at wave and tidal energy sites in orkney, scotland. *IEEE Journal of Oceanic Engineering 41*, 1 (2016), 67–81.